Inorganic Chemistry

Article

pubs.acs.org/IC

Intramolecular Phosphorus−Phosphorus Bond Formation within a Co_2P_4 Core

Tianshu Li,[†] Nicholas Arleth,[†] Michael T. Gamer,[†] Ralf Köppe,[†] Timo Augenstein,[†] Fabian Dielmann,[‡] Manfred Scheer,[‡] Sergey N. Konchenko,[†,§] and Peter W. Roesky*[,†]

[†]Institute of Inorganic Chemistry, Karlsruhe Institute of Technology, 76131 Karlsruhe, Germany

[‡]Institute of Inorganic Chemistry, University of Regensburg, 93040 Regensburg, Germany

[§]Nikolaev Institute of Inorganic Chemistry, Siberian Branch of Russian Academy of Sciences, Prosp. Lavrentieva 3, 630090 Novosibirsk, Russia

Supporting Information

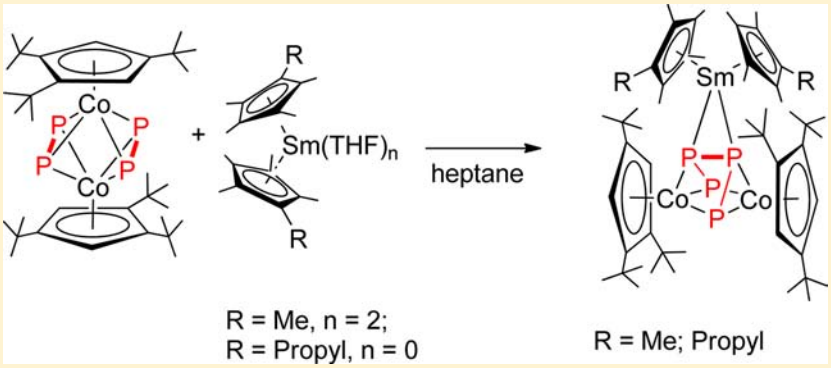

ABSTRACT: The reduction of $[(Cp'''Co)_2(\mu,\eta^{2:2}\text{-}P_2)_2]$ (Cp''' = 1,2,4-tBu$_3$C$_5$H$_2$) with the samarocenes, $[(C_5Me_4R)_2Sm(THF)_n]$ (R = Me or n-propyl), gives $[(Cp'''Co)_2P_4Sm(C_5Me_4R)_2]$. This is the first example of an intramolecular P−P coupling in a polyphosphide complex upon reduction of the transition metal. The formation of the P−P bond is not a result of the direct reduction of the phosphorus atoms but is induced by a rearrangement of the positive charges between the metal atoms.

INTRODUCTION

Since Kagan and co-workers reported the divalent samarium reagent SmI_2 as a single-electron reducing agent in 1980,[1] many other examples of carbon−carbon bond formation by SmI_2 have been established.[2] The commonly accepted mechanisms of SmI_2-mediated reactions anticipate radical species as intermediates.[2a] Because phosphorus atoms termed a "carbon copy" are isolobal to a CH fragment,[3] we and others investigated the reaction of divalent samarium and related compounds that yields phosphorus−phosphorus bonds. Thus, in 2009, the divalent solvate-free samarocene $[Cp^*_2Sm]$ (Cp^* = η^5-C_5Me_5) was used to synthesize the first molecular rare-earth metal polyphosphide, $[(Cp^*_2Sm)_4P_8]$.[4] The structure can be described as a realgar-shaped P_8^{4-} ligand trapped in a cage of four samarocenes. $[(Cp^*_2Sm)_4P_8]$ is formed by the transfer of one electron from each divalent samarium atom to the phosphorus scaffold. Another example of direct activation of P_4 to P_8^{4-} ligand stabilized by a scandium naphthalene complex has recently been reported.[5] The first well-defined P^{3-}-containing rare-earth metal compounds in which six yttrium atoms coordinate to the μ_6-P^{3-} ligand have been described.[6] The reductive dimerization of the phosphaalkyne tBuC≡P can be achieved by $[Cp^*_2Sm]$ and a divalent porphyrinogen samarium complex.[7] tBuC≡P can also be reduced in an electron beam-vaporized scandium system by co-condensation to form the low-valent scandium 1,3,5-triphosphabenzene complex, $[\{(\eta^5\text{-}P_3C_2t\text{Bu}_2)Sc\}_2(\mu\text{-}\eta^6\text{:}\eta^6\text{-}P_3C_3t\text{Bu}_3)]$.[8] Recently, we reported on the reactions of divalent samarium compounds with transition metal-coordinated polyphosphides.[9] In this context, the first formation of a P−P bond between two $[Cp^*FeP_5]$ molecules triggered by divalent lanthanide complexes to give $[(Cp^*Fe)_2P_{10}\{Sm(\eta^5\text{-}C_5Me_4R)_2\}_2]$ (R = Me or nPr) was reported. This intermolecular P−P bond formation is due to two-electron reductive dimerization.[9a,10]

One of the unique electronic properties of phosphorus is the formation of phosphorus−phosphorus odd-electron bonds by means of a π^*−π^* interaction.[11] Because divalent lanthanide complexes are one-electron reducing reagents, we are interested in extending our studies of P−P bond formation of transition metal-coordinated polyphosphides by using only 1 equiv of the lanthanide reagent. Here, we choose a cobalt polyphosphide complex, $[\{Cp'''Co(\mu,\eta^{2:2}\text{-}P_2)\}_2]$ (Cp''' = 1,2,4-tBu$_3$C$_5$H$_2$), as a starting complex, which was originally reported as a Cp^* derivative by Barr and Dahl in 1991 and synthesized by a low-yield reaction of $[Cp^*Co(\mu\text{-}CO)_2]$ with P_4 upon photolysis in

Received: August 23, 2013
Published: December 5, 2013

   dx.doi.org/10.1021/ic402159y | Inorg. Chem. 2013, 52, 14231−14236

toluene.[12] Scheer's group reported in 2010 the quantitative synthesis of $[(Cp'''Co)_2(\mu,\eta^{2:2}\text{-}P_2)_2]$ by using $[(Cp'''Co)_2(\mu,\eta^{4:4}\text{-}C_7H_8)]$ as a precursor, which also affords access to extended polyphosphorus frameworks.[13] Radius and co-workers recently performed a systematic study of the degradation of symmetrical P_4 to P_2 units bridging two cobalt atoms.[14] The reaction of the olefin cobalt N-heterocyclic carbene complex $[Cp^*Co(iPr_2Im)(\eta^2\text{-}C_2H_4)]$ (iPr_2Im = 1,3-diisopropylimidazolin-2-ylidene) with P_4 gave in two steps the dinuclear complex $[\{Cp^*Co(iPr_2Im)\}_2(\mu,\eta^{2:2}\text{-}P_4)]$. The dissociation of both N-heterocyclic carbene ligands yielded the dinuclear bis(diphosphide)-bridged complex $[\{Cp^*Co(\mu,\eta^{2:2}\text{-}P_2)\}_2]$.[14]

EXPERIMENTAL SECTION

General Considerations. All manipulations of air-sensitive materials were performed with the rigorous exclusion of oxygen and moisture in flame-dried Schlenk-type glassware either on a dual manifold Schlenk line, interfaced to a high-vacuum (10^{-3} Torr) line, or in an argon-filled MBraun glovebox. Nuclear magnetic resonance (NMR) spectra were recorded on a Bruker Avance 400 MHz or Bruker Avance II 300 MHz NMR spectrometer. Chemical shifts are referenced to internal solvent resonances and are reported relative to tetramethylsilane (^{1}H NMR) and 85% phosphoric acid (^{31}P NMR). IR spectra (Figures S1 and S2 of the Supporting Information) were obtained on a Bruker Tensor 37 Fourier transform infrared (FTIR) spectrometer. Elemental analyses were conducted with an Elementar vario EL or micro cube instrument. Ether solvents (THF and Et_2O) and hydrocarbon solvents (toluene, heptane, and *n*-pentane) were predried by using an MBraun solvent purification system (SPS-800) and degassed, dried, and stored *in vacuo* over Na/K alloy benzophenone ketyl in resealable flasks prior to use. Deuterated solvents were obtained from Aldrich (99 atom % D) and were degassed, dried, and stored *in vacuo* over Na/K alloy in resealable flasks. $[(Cp'''Co)_2(\mu,\eta^{2:2}\text{-}P_2)_2]$ (Cp''' = 1,2,4-tBu$_3$C$_5$H$_2$),[12,13,15] $[Cp^*_2Sm(THF)_2]$,[16] and $[(C_5Me_4nPr)_2Sm]$[17] were prepared according to literature procedures.

General Procedure for Ampule Reactions. For the synthesis and recrystallization, two-section ampules were used. The starting compounds were loaded in one section of the ampule in an Ar glovebox. The section with loading was cooled with liquid nitrogen, and the corresponding solvent (typically 10 mL of solvent) was condensed in vacuum with the mixture of starting material. The ampule was flame-sealed. The reaction mixture was slowly warmed to room temperature, stirred for 14 h, and heated to 60 °C until the color had definitely changed from purple to red-brown. In the case of the formation of a precipitate, it will be separated by decantation of the solution to another section of the ampule. The concentrated solution was obtained by slow evaporation of the solvent to the empty section of the ampule. The section with the solvent and precipitate was removed by flame sealing. The crystals were obtained by cooling the concentrated solution in a freezer (−11 °C), decanting the solution to the other end of ampule, and drying by means of cooling the section with the mother liquid. The section with crystals was flame-sealed and opened in a glovebox.

Electrochemistry. Cyclic voltammetry measurements were performed with an EG&G potentiostat (PAR model 263A) and an electrochemical cell for sensitive compounds. We used a freshly polished Pt disk working electrode, a Pt wire as the counter electrode, and a Ag wire as a (pseudo) reference electrode [$[n$Bu$_4$N$][PF_6]$ (0.1 M) as the electrolyte]. Potentials were calibrated against the Fc/Fc^+ couple, which has a potential ($E^0_{1/2}$) of 0.35 V versus Ag/AgCl (Figure S5 of the Supporting Information).

Near-Infrared Absorbance (NIR) Measurements of 1a and 1b. NIR measurements of **1a** and **1b** were performed with the help of an ATR diamond at room temperature using the Bruker Tensor 37 FTIR spectrometer by means of a NIR lamp, a CaF_2 beam splitter, and a room-temperature InGaAs detector (Figures S3 and S4 of the Supporting Information).

Synthesis of 1a and 1b. *$[Cp^*_2SmP_4(CoCp'''_2]$ (**1a**).* Heptane (10 mL) was condensed onto a mixture of $[Cp^*_2Sm(THF)_2]$ (0.104 g, 0.18 mmol) and $[(Cp'''Co)_2(\mu,\eta^{2:2}\text{-}P_2)_2]$ (0.130 g, 0.18 mmol) cooled to −78 °C. The resulting reaction mixture was stirred for 16 h at 60 °C. The mixture was filtered off into a two-section ampule to grow crystals by slow evaporation. The purple crystals of **1a**·$^1/_2$heptane were obtained at ambient temperature after slow concentration of the solution: yield 0.164 g (77%); MIR (ATR, ν) 2958 (vs), 2909 (s), 2866 (s), 1485 (m), 1458 (m), 1393 (m), 1360 (m), 1247 (m), 1167 (m), 1023 (m), 994 (m), 945 (m), 830 (m), 571 (br, m), 504 (m) cm^{-1}; NIR (ATR, ν) 9257 ($^6F_{9/2}$), 7999 ($^6F_{7/2}$), 7288 ($^6F_{5/2}$), 6355 ($^6F_{1/2}$) cm^{-1}. Anal. Calcd for **1**·$^1/_2$heptane, $C_{57.5}H_{96}Co_2P_4Sm$: C, 58.55; H, 8.20. Found: C, 58.59; H, 8.35.

*$[(C_5Me_4nPr)_2SmP_4(CoCp'''_2]$ (**1b**).* Heptane (10 mL) was condensed onto a mixture of $[(C_5Me_4nPr)_2Sm]$ (0.127 g, 0.27 mmol) and $[(Cp'''Co)_2(\mu,\eta^{2:2}\text{-}P_2)_2]$ (0.146 g, 0.2 mmol) cooled to −78 °C. The resulting reaction mixture was stirred for 16 h at 60 °C. The small volume of solvent was removed and cooled to −25 °C, resulting in the formation of a dark solid. The solid was extracted with pentane (5 mL), and the solution was filtered into a two-section ampule to grow crystals by slow evaporation. The purple crystals were obtained at −25 °C within a few days: yield 0.140 g (56%); MIR (ATR, ν) 2955 (vs), 2916 (s), 2866 (s), 1484 (w), 1455 (m), 1388 (w), 1361 (m), 1244 (m), 1166 (m), 1052 (br, m), 1022 (m), 994 (m), 944 (m), 859 (w), 830 (m), 565 (br, m), 501 (m) cm^{-1}; NIR (ATR, ν) 9235 ($^6F_{9/2}$), 7985 ($^6F_{7/2}$), 7270 ($^6F_{5/2}$), 6798 ($^6F_{3/2}$), 6340 ($^6F_{1/2}$) cm^{-1}. Anal. Calcd for **1b**, $C_{58}H_{94}Co_2P_4Sm$: C, 58.86; H, 8.01. Found: C, 58.82; H, 8.08.

X-ray Crystallographic Studies of 1a and 1b. A suitable crystal was covered in mineral oil (Aldrich) and mounted on a glass fiber. The crystal was transferred directly to the −73 or −123 °C cold stream of a STOE IPDS 2 diffractometer.

All structures were determined by the Patterson method (SHELXS-97[18]). The remaining non-hydrogen atoms were located via the successive difference in Fourier map calculations. The refinements were conducted using full-matrix least-squares techniques on F, minimizing the function $(F_o - F_c)^2$, where the weight is defined as $4F_o^2/2(F_o^2)$ and F_o and F_c are the observed and calculated structure factor amplitudes, respectively, using SHELXL-97.[18] Carbon-bound hydrogen atom positions were calculated. The final values of refinement parameters are listed in Table 1. The locations of the largest peaks in the final difference Fourier map calculation as well as the magnitude of the residual electron densities in each case were of no chemical significance. Positional parameters, hydrogen atom parameters, thermal parameters, and bond distances and angles have been deposited as Supporting Information.

Crystallographic data (excluding structure factors) for the structures reported in this paper have been deposited with the Cambridge Crystallographic Data Centre as supplementary publication CCDC 937045-937047. Copies of the data can be obtained free of charge on application to CCDC, 12 Union Road, Cambridge CB21EZ, U.K. [fax +(44)1223-336-033, e-mail deposit@ccdc.cam.ac.uk].

Quantum Chemical Density Functional Theory (DFT) Calculations. The quantum chemical RI-DFT calculations were performed with TURBOMOLE[19] by using the BP86 functional[20] and the RI-J approximation.[21] The basis sets for C, H, P, and K were of def2-QZVP quality.[22] For the 4f^5 subconfiguration of Sm^{3+}, a relativistic corrected effective core potential has been used to simulate the 51 inner electrons (ECP-51).[23] It has been shown that for the rare-earth metals an inclusion of the partially occupied 4f orbitals in the core and the treatment of different f occupations by diverse pseudopotentials offer the possibility of performing quantum chemical calculations on lanthanide compounds within a reasonable amount of computer time. Sm of the +III formal oxidation state is undoubtedly expected because of the ionic nature of the complex.[24] As a consequence, the 4f^5 subconfiguration of the ECP-treated Sm^{3+} is not part of the notation of the electronic state of

dx.doi.org/10.1021/ic402159y | Inorg. Chem. 2013, 52, 14231−14236

Table 1. Crystallographic Details of 1a and 1b

	1a	1a·C_6H_{14}	1b
chemical formula	$C_{54}H_{88}Co_2P_4Sm$	$C_{54}H_{88}Co_2P_4Sm\cdot C_6H_{14}$	$C_{58}H_{96}Co_2P_4Sm$
formula mass	1129.33	1215.51	1185.44
crystal system	triclinic	monoclinic	triclinic
a (Å)	13.0834(5)	10.3372(3)	13.0764(14)
b (Å)	14.3533(6)	17.1314(5)	14.5320(14)
c (Å)	19.3890(8)	34.8910(11)	17.9246(19)
α (deg)	68.837(3)		75.202(8)
β (deg)	81.074(3)	97.782(2)	84.017(9)
γ (deg)	63.807(3)		63.168(7)
unit cell volume (Å^3)	3046.8(2)	6122.0(3)	2938.4(5)
temperature (K)	200(2)	150(2)	150(2)
space group	$P\bar{1}$	$P2_1/c$	$P\bar{1}$
no. of formula units per unit cell (Z)	2	4	2
no. of reflections measured	23125	26465	22333
R_{int}	0.0330	0.0937	0.0969
final R_1 values [$I > 2\sigma(I)$]	0.0307	0.0390	0.0661
final $wR(F^2)$ values [$I > 2\sigma(I)$]	0.0450	0.0813	0.1396
final R_1 values (all data)	0.0512	0.0607	0.1485
final $wR(F^2)$ values (all data)	0.0469	0.0864	0.1746

$[Co_2Cp_2P_4]^-[SmCp_2]^+$ (^{2}B, see the note of Table S1 of the Supporting Information).

The geometry optimizations were conducted with the help of analytically derived gradients using redundant internal coordinates.[25] Theoretical vibrational spectra were obtained by calculation of the second derivatives using the module AOFORCE[26] to prove that the structures belong to energy minima and not to saddle points. Results of the quantum chemical DFT calculations are listed in Table S1 of the Supporting Information.

RESULTS AND DISCUSSION

Herein, we report an intramolecular P−P coupling in the polyphosphide complex by a divalent lanthanide complex. The reaction of $[(Cp'''Co)_2(\mu,\eta^{2:2}\text{-}P_2)_2]$ with the THF adduct of decamethylsamarocene, $[Cp^*_2Sm(THF)_2]$, or the solvent-free di(tetramethyl-*n*-propyl)samarocene, $[(C_5Me_4(n\text{-}propyl))_2Sm]$,[9a,17] was conducted in heptane at an elevated temperature (Scheme 1). Dark brown crystals of $[(Cp'''Co)_2P_4Sm(\eta^5\text{-}C_5Me_4R)_2]$ [R = Me (**1a**) or *n*-propyl (**1b**)] were formed in a saturated hexane or heptane solution by slow evaporation. Trinuclear complexes **1a** and **1b** were characterized by analytical and spectroscopic methods. The oxidation state of the samarium atom in **1a** and **1b** was determined by NIR spectroscopy, which exhibited a characteristic absorbance pattern for Sm(III) complexes. Therefore, the formation of an acyclic P_4 bridge among the three metals in **1a** and **1b** was initiated by the transfer of one electron from the samarocene to $[(Cp'''Co)_2(\mu,\eta^{2:2}\text{-}P_2)_2]$. Even though Winter and Geiger examined the quasi-reversible one-electron oxidation process of $[\{Cp'''Co(\mu,\eta^{2:2}\text{-}P_2)\}_2]$ to $[\{Cp'''Co(P_2)\}_2]^+$ ($E^0_{1/2}$ = 0.33 V) by cyclic voltammetry,[27] one-electron reduction of this dicobalt $\mu,\eta^{2:2}$-polyphosphide complex has not been reported. For this reason, we performed cyclic voltammetry studies of the one-electron reduction process. For $[\{Cp'''Co(\mu,\eta^{2:2}\text{-}P_2)\}_2]$, we found that the complex can be quasi-reversibly reduced to $[\{Cp'''Co(P_2)\}_2]^-$ at a potential ($E^0_{1/2}$) of −1.77 V in THF. Accordingly, the reduction potential of divalent samarocene [$E^0_{1/2}(Sm^{2+})$ = −2.12 V][28] is sufficiently reductive for the dicobalt complex.

The solid state structures of **1a** and **1b** were established by single-crystal X-ray diffraction (Figures 1 and 2). On the basis of the solvent used in growing the crystals, **1a** crystallizes in two different space groups ($P\bar{1}$ and $P2_1/c$ with hexane in the unit cell). Compound **1b** was crystallized from heptane in space group $P\bar{1}$. Complexes **1a** and **1b** present a distorted trigonal prismatic geometry in a Co_2P_4 core (Figure 1). A noncrystallographic C_2 axis is observed along Sm and the center of the P_2Co_2 plane of the trigonal prism. Because of the structure of the trigonal prism, **1a** and **1b** have an axial chirality, but as a result of the centrosymmetric space groups, both enantiomers are observed in the unit cell. The Λ-**1a** enantiomer crystallized from hexane and the Δ-**1a** enantiomer crystallized from heptane are shown in Figure 1. A similar trigonal prismatic framework was reported in a Ni_2P_4 core of $[(Cp^{pr}Ni)_2P_4(W(CO)_5)_2]$[29] ($Cp^{pr}$ = $C_5H(iPr)_4$) or $[(Cp^*Ni)_2P_4(Cr(CO)_5)_2]$[30] formed by the P_4 activation reaction in the presence of nickel carbonyl complex $[Cp^{pr}Ni(CO)]_2$ or $[Cp^*Ni(CO)]_2$ and $[M(CO)_5]$ (M = W or Cr).

The formation of the distorted trigonal prism in **1a** and **1b** forces the originally parallel Cp‴ planes in $[\{Cp'''Co(\mu,\eta^{2:2}\text{-}P_2)\}_2]$ to angles of 62.52° and 63.3° in **1a** and 63.30° in **1b**. The two cobalt atoms are situated at the diagonal vertices of the basal rectangle in the prism with Co−Co distances of 3.004(3)

Scheme 1

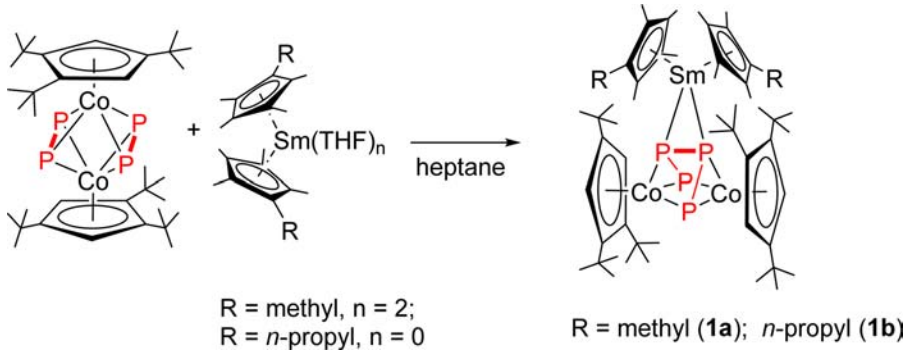

dx.doi.org/10.1021/ic402159y | Inorg. Chem. 2013, 52, 14231−14236

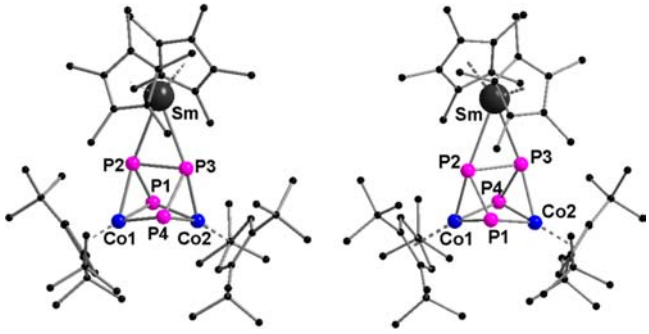

Figure 1. Solid-state structures of Λ-**1a** crystallized from hexane (left) and Δ-**1a** crystallized from heptane (right). Hydrogen atoms have been omitted for the sake of clarity. Selected bond lengths (angstroms) and angles (degrees) in Λ-**1a**: P1−P2, 2.149(1); P2−P3, 2.241(2); P3−P4, 2.150(2); Co1−P1, 2.2751(12); Co1−P2, 2.2638(13); Co1−P4, 2.2305(11); Co2−P1, 2.2304(10); Co2−P3, 2.2596(12); Co2−P4, 2.2688(12); Sm−P2, 2.9153(11); Sm−P3, 2.9027(11); P1···P4, 3.261(2); Co1···Co2, 2.982(2); P3−Sm−P2, 45.44(3); P1−P2−P3, 83.84(5); P4−P3−P2, 84.88(5). Selected bond lengths (angstroms) and angles (degrees) in Δ-**1a**: P1−P2, 2.1485(11); P2−P3, 2.2529(11); P3−P4, 2.1501(12); Co1−P1, 2.2791(9); Co1−P2, 2.2485(9); Co1−P4, 2.2339(9); Co2−P1, 2.2295(9); Co2−P3, 2.2572(9); Co2−P4, 2.2765(9); Sm−P2, 2.8856(8); Sm−P3, 2.9267(8); P1···P4, 3.257(4); Co1···Co2, 3.004(3); P2−Sm−P3, 45.60(2); P1−P2−P3, 84.17(4); P4−P3−P2, 84.22(4).

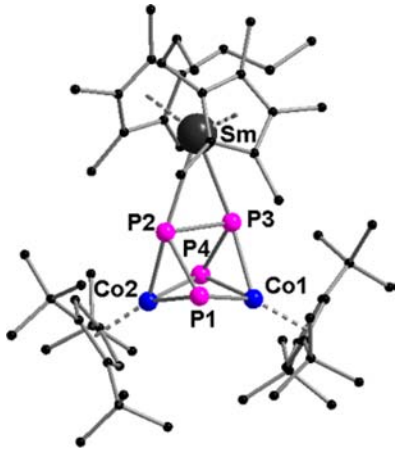

Figure 2. Solid-state structure of **1b**. Hydrogen atoms have been omitted for the sake of clarity. Selected bond lengths (angstroms) and angles (degrees): P1−P2, 2.154(4); P2−P3, 2.251(4); P3−P4, 2.160(4); P1−Co1, 2.232(3); P3−Co1, 2.259(3); P4−Co1, 2.288(3); P1−Co2, 2.272(3); P2−Co2, 2.265(3); P4−Co2, 2.228(4); P3−Sm, 2.874(3); P2−Sm, 2.921(3); P1···P4, 3.278(12); Co1···Co2, 2.982(2); P3−Sm−P2, 45.70(9); P1−P2−P3, 84.66(14); P4−P3−P2, 84.6(2).

Å in **1a** and 2.982(1) Å in **1b**, which are shortened from the Co−Co nonbonding distance of 3.164 Å in the starting dicobalt complex.[15] Two nearly isosceles triangles are composed of two phosphorus atoms and one cobalt atom each with P−P bond distances ranging from 2.149(1) to 2.150(2) Å, which are elongated compared to the double-bond distance of 2.052(2) Å in $[\{Cp'''Co(\mu,\eta^{2:2}\text{-}P_2)\}_2]$ but still shorter than a P−P single-bond distance of 2.194 Å in P_4.[31,32] The newly formed P2−P3 bond with a distance of 2.241(2) Å (**1a**) or 2.253(3) Å (**1b**) links the two triangles and bridges the samarium and cobalt atoms. The Sm−P bonds are in the range of 2.874(3) and 2.926(2) Å and slightly shorter than the Sm−P bonds in $[(Cp^*_2Sm)_4P_8]$.[4] The Cg−Sm (Cg = Cp*-ring centroid) distances and the Cg−Sm−Cg angles are in the expected ranges of trivalent samarocene complexes.[33]

Another P−P bond coupling between the two P_2 units to a P_4 unit in $[(Cp'''Co)_2(P_4)M(CO)_5]$ (M = Mo or W) was reported by Scherer and co-workers.[15,34] Although both the example of Scherer and our example were formed by metal-induced intramolecular P−P coupling on $[\{Cp'''Co(\mu,\eta^{2:2}\text{-}P_2)\}_2]$, the two resulting P_4 systems are very different in terms of their geometry and bonding properties. As shown in Scheme 2, terminal coordination of a $M(CO)_5$ unit to $[\{Cp'''Co(\mu,\eta^{2:2}\text{-}P_2)\}_2]$ led to a P−P bond formation with minimal geometric changes from the starting dicobalt complex. The tetraphosphorus scaffold in the neutral molybdenum- or tungsten-coordinated complexes, $[(Cp'''Co)_2(P_4)M(CO)_5]$, is planar and rectangularly arranged, while in **1a** or **1b**, it is twisted and nonplanar. Because of the terminal coordination of the molybdenum or tungsten carbonyl fragments to one of the phosphorus atoms of $[\{Cp'''Co(\mu,\eta^{2:2}\text{-}P_2)\}_2]$, the two P_2 units move close to each other. This was described by the authors as the formation of a new but very long P−P bond, e.g., 2.385(5) Å in $[(Cp'''Co)_2(P_4)W(CO)_5]$.[15] In contrast, the newly formed P−P (P2−P3) bond in **1a** or **1b**, which is side-on-bonded to the Sm(III) metal atom, is ∼0.13 Å shorter than the P−P bond mentioned above and, thus, in the expected range of a P−P single bond.[31,32,35] On the basis of the comparisons, the electronic properties of these two systems are very different, and the one-electron transfer from the divalent samarocene starting material to the Co_2P_4 framework plays an important role in the transformation from P_2 to P_4 in **1a** and **1b**. However, the P2−P3 bond length ranging between 2.241(2) and 2.253(3) Å represents a classic P−P single-bond distance and is much shorter than the first reported one-electron P−P bond distance of 2.634 Å.[11g] The new bond appears to be formed by rearrangement of P−P double bonds in $[\{Cp'''Co(\mu,\eta^{2:2}\text{-}P_2)\}_2]$ triggered by one-electron reduction of Co by samarocene. The similarity of the Co−P bond distances in a range from 2.230(3) to 2.288(3) Å in **1a** and **1b** suggests that the single electron is probably delocalized in the Co_2P_4 frameworks. The calculated spin density distribution and further computational details are outlined in the theoretical section below. The fact that $^{31}P\{^1H\}$

Scheme 2

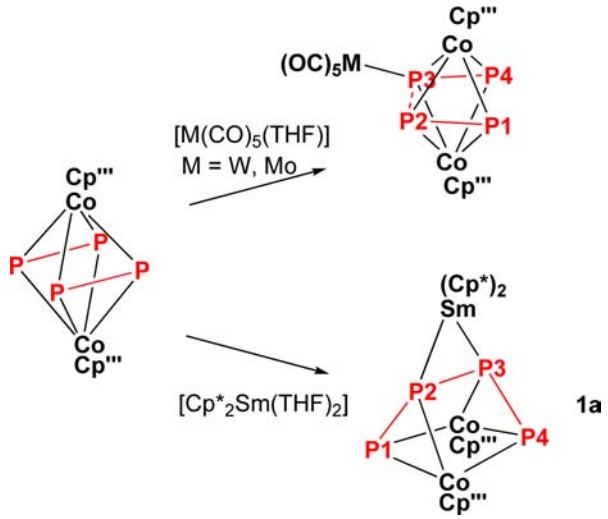

dx.doi.org/10.1021/ic402159y | Inorg. Chem. 2013, 52, 14231−14236

NMR spectra of the crystals of **1a** and **1b** dissolved in THF show only a singlet with a chemical shift similar to that of the starting material $[\{Cp'''Co(\mu,\eta^{2:2}\text{-}P_2)\}_2]$ suggests that **1a** and **1b** are unstable in THF solution and slowly decompose.

Density functional theory calculations were performed to understand the structural change of the $(P_2)_2$ unit in $[\{Cp'''Co(\mu,\eta^{2:2}\text{-}P_2)\}_2]$ after the formation of **1a**. Instead of the complete molecules, we investigated model compounds $[\{CpCo(\mu,\eta^{2:2}\text{-}P_2)\}_2]$ and $[Cp_2SmP_4(CoCp)_2]$ as well as $K[P_4(CoCp)_2]$ simulating a complete charge transfer to the starting molecule.[36] This approach is valid, although differences especially for the nonbonded P−P distances are expected because of the comparison of molecules in different phases and with different ligands. One striking feature is the reduced local symmetry of the Co_2P_4 unit in $[\{CpCo(\mu,\eta^{2:2}\text{-}P_2)\}_2]$ in the calculation (C_{2v}) with respect to the experiment (D_{2h}). With regard to the precursor model substance $[\{CpCo(\mu,\eta^{2:2}\text{-}P_2)\}_2]$, we agree with Radius et al. that the cobalt atom is in the formal oxidation state +III formal oxidation state and each P_2 is best described as a dianion.[14] This finding is in line with the comparison of calculated P−P distances, r(P−P), in $[\{CpCo(\mu,\eta^{2:2}\text{-}P_2)\}_2]$ and P_2^{2-} of 2.093 and 2.120 Å, respectively (Table S1 of the Supporting Information). As a result of the analysis of the valence MOs in $[\{CpCo(\mu,\eta^{2:2}\text{-}P_2)\}_2]$ (see the Supporting Information), we find a certain $\pi^*-\pi^*$ interaction between the two P_2^{2-} units explaining their weak aggregation similar to that in $[I_4]^{2+}$. Via comparison of bonded and formally nonbonded P···P distances in this model compound [r(P1−P2) = 2.093 Å, r(P2···P3) = 2.457 Å, and r(P1···P4) = 2.906 Å] with the situation of the two I_2^+ units in $[I_4]^{2+}$ [r(I−I) = 2.58 Å, and r(I···I) = 3.37 Å[37]], aggregation in the $2P_2^{2-}/P_4^{4-}$ system appears even stronger. The geometric parameters of model compounds $[Cp_2SmP_4(CoCp)_2]$ and $K[P_4(CoCp)_2]$ nicely agree with the experimental observations of **1a**; as a consequence, we believe that the trigonal prismatic shape of the Co_2P_4 core in title compound **1a** is not due to steric effects but electronic effects.[38] With the help of Mulliken population analyses, the partial charges of the $SmCp_2$ and K units are determined to be +0.22 and +0.76, respectively. In both model compounds, the spin density resides completely on the cobalt atoms.[39] To obtain insight into the changes after formation of the reduced compound, we compared the MO diagrams and isosurfaces of the MOs with a pronounced P contribution of $[\{CpCo(\mu,\eta^{2:2}\text{-}P_2)\}_2]$ (C_{2v} symmetry) with those of $K[P_4(CoCp)_2]$ (C_2 symmetry) (Figure 3 and the Supporting Information). One finds the following qualitative changes: π-MO 12 a_2 changes into MO 47 a with certain Co−Co interaction, whereas the π-type in-plane interaction in MOs 28 and 31 a_1 change to MOs 44 and 52 a. These MOs are responsible for the formation of a weak bond between P2 and P3 by twisting of the two P_2 units with respect to the C_2 axis of the model compound. The best view from their animated isosurface plots is given in Figure S1 of the Supporting Information.

As the partial charge on the P_4 unit (−1.66) in $[\{CpCo(\mu,\eta^{2:2}\text{-}P_2)\}_2]$ is the same size as that on reduced model compound $[Cp_2SmP_4(CoCp)_2]$ (−1.38), we assign the polyphosphide ligand as P_4^{4-} formed from two P_2^{2-} units after rearrangement of the positive charges: on one hand two $[CoCp]^{2+}$ units in $[\{CpCo(\mu,\eta^{2:2}\text{-}P_2)\}_2]$ and on the other hand a $[CoCp]^+$, a $[CoCp]^{2+}$, and a K^+ or $[SmCp_2]^+$ unit in $K[P_4(CoCp)_2]$ or $[Cp_2SmP_4(CoCp)_2]$, respectively. The dimerization of the two P_2^{2-} ligands to form P_4^{4-} appears to be comprehensible as the dimerization of two isoelectronic S_2 molecules forming S_4 for which a heat of reaction of −26.5 kcal/mol[40] was found experimentally. Furthermore, $\pi^*-\pi^*$ interaction in the comparable system I_4^{2+}, in which its cyclic tetragonal I_4^{2+} features through-space in-plane conjugation, is calculated to have an energy only ∼2.4 kcal/mol lower than that of its acyclic C_{2h}-symmetric isomer.[37] The calculation suggests that the bonding situation in model compound $[(CpCo)_2(P_4)W(CO)_5]$ is different. Upon coordination of $W(CO)_5$, the principal shape of the molecule remains almost unchanged and interaction between both P_2 units remains weak. This is consistent with the findings of extended Hückel calculations (EHT) on $[CpCo(P_4)\{(CpCo)_2(\mu\text{-}CO)\}]$.[41]

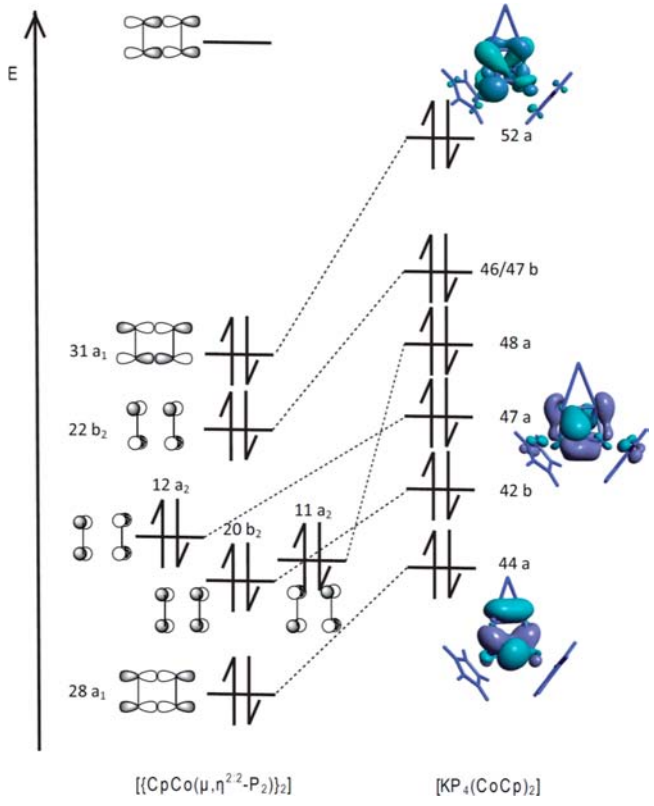

Figure 3. MO diagram describing the changes after reaction of model compound $[\{Cp'''Co(\mu,\eta^{2:2}\text{-}P_2)\}_2]$ with K. On the left, only those MOs with a pronounced P contribution are given (see Figure S1 of the Supporting Information for a detailed description by animated orbitals; values of the isosurfaces of ±0.04).

■ CONCLUSIONS

In conclusion, we have prepared and fully characterized two polyphosphide bridging 3d/4f metal complexes, $[(Cp'''Co)_2P_4Sm(C_5Me_4R)_2]$ [R = Me (**1a**), or R = *n*-propyl (**1b**)]. They represent the first examples of an intramolecular P−P coupling in a polyphosphide complex after reduction of the transition metal by a divalent lanthanide complex.[42] The formation of the P−P bond is not a result of the direct reduction of the phosphorus atoms. Instead, the spin density is entirely localized on the cobalt atoms. The formal transfer of the positive charge from the cobalt to the samarium atom leads to a redistribution of the local charges in the $\{Co(\mu,\eta^{2:2}\text{-}P_2)\}_2$ scaffold. As a result, the two P_2^{2-} ligands aggregated by weak $\pi^*-\pi^*$-type interaction rearrange to an acyclic $[P_4]^{4-}$ entity with a newly formed P−P bond. We thus have elucidated a rare

dx.doi.org/10.1021/ic402159y | Inorg. Chem. 2013, 52, 14231−14236

case of P−P bond formation that is not triggered by a direct reduction but by a rearrangement of the positive charges between two metal atoms.

■ ASSOCIATED CONTENT

Supporting Information

Additional tables and figures and CIF data. This material is available free of charge via the Internet at http://pubs.acs.org.

■ AUTHOR INFORMATION

Corresponding Author

*E-mail: roesky@kit.edu.

Notes

The authors declare no competing financial interest.

■ ACKNOWLEDGMENTS

This work was supported by the Deutsche Forschungsgemeinschaft (DFG), the Russian Foundation for Basic Research (RFBR), and the Landesstiftung Baden-Württemberg GmbH. F.D. thanks the Studienstiftung des deutschen Volkes for a Ph.D. scholarship. Prof. F. Breher is acknowledged for helpful discussions.

■ REFERENCES

(1) Girard, P.; Namy, J. L.; Kagan, H. B. *J. Am. Chem. Soc.* **1980**, *102*, 2693.

(2) (a) Nicolaou, K. C.; Ellery, S. P.; Chen, J. S. *Angew. Chem., Int. Ed.* **2009**, *48*, 7140. (b) Beemelmanns, C.; Reissig, H.-U. *Chem. Soc. Rev.* **2011**, *40*, 2199. (c) Molander, G. A. *Chem. Rev.* **1992**, *92*, 29.

(3) Dillon, K. B.; Mathey, F.; Nixon, J. F. *Phosphorus: The Carbon Copy*; Wiley: Chichester, U.K., 1998.

(4) Konchenko, S. N.; Pushkarevsky, N. A.; Gamer, M. T.; Köppe, R.; Schnöckel, H.; Roesky, P. W. *J. Am. Chem. Soc.* **2009**, *131*, 5740.

(5) Huang, W.; Diaconescu, P. L. *Chem. Commun.* **2012**, *48*, 2216.

(6) Lv, Y.; Xu, X.; Chen, Y.; Leng, X.; Borzov, M. V. *Angew. Chem., Int. Ed.* **2011**, *50*, 11227.

(7) (a) Gardiner, M. G.; James, A. N.; Jones, C.; Schulten, C. *Dalton Trans.* **2010**, *39*, 6864. (b) Recknagel, A.; Stalke, D.; Roesky, H. W.; Edelmann, F. T. *Angew. Chem., Int. Ed.* **1989**, *28*, 445.

(8) Arnold, P. L.; Cloke, F. G. N.; Hitchcock, P. B.; Nixon, J. F. *J. Am. Chem. Soc.* **1996**, *118*, 7630.

(9) (a) Li, T.; Gamer, M. T.; Scheer, M.; Konchenko, S. N.; Roesky, P. W. *Chem. Commun.* **2013**, *49*, 2183. (b) Li, T.; Wiecko, J.; Pushkarevsky, N. A.; Gamer, M. T.; Köppe, R.; Konchenko, S. N.; Scheer, M.; Roesky, P. W. *Angew. Chem., Int. Ed.* **2011**, *50*, 9491.

(10) For the reductive dimerization, see: Butovskii, M. V.; Balázs, G.; Bodensteiner, M.; Peresypkina, E. V.; Virovets, A. V.; Scheer, M. *Angew. Chem., Int. Ed.* **2013**, *52*, 2972.

(11) (a) Soleilhavoup, M.; Bertrand, G. *Bull. Chem. Soc. Jpn.* **2007**, *80*, 1241. (b) Kato, T.; Gornitzka, H.; Schoeller, W. W.; Baceiredo, A.; Bertrand, G. *Angew. Chem., Int. Ed.* **2005**, *44*, 5497. (c) Choua, S.; Dutan, C.; Cataldo, L.; Berclaz, T.; Geoffroy, M.; Mézailles, N.; Moores, A.; Ricard, L.; Le Floch, P. *Chem.—Eur. J.* **2004**, *10*, 4080. (d) Cataldo, L.; Choua, S.; Berclaz, T.; Geoffroy, M.; Mézailles, N.; Ricard, L.; Mathey, F.; Floch, P. L. *J. Am. Chem. Soc.* **2001**, *123*, 6654. (e) Kato, T.; Gornitzka, H.; Baceiredo, A.; Schoeller, W. W.; Bertrand, G. *Science* **2000**, *289*, 754. (f) Grützmacher, H. *Science* **2000**, *289*, 737. (g) Canac, Y.; Bourissou, D.; Baceiredo, A.; Gornitzka, H.; Schoeller, W. W.; Bertrand, G. *Science* **1998**, *279*, 2080. (h) Grützmacher, H.; Breher, F. *Angew. Chem., Int. Ed.* **2002**, *41*, 4006.

(12) Barr, M. E.; Dahl, L. F. *Organometallics* **1991**, *10*, 3991.

(13) Dielmann, F.; Sierka, M.; Virovets, A. V.; Scheer, M. *Angew. Chem., Int. Ed.* **2010**, *49*, 6860.

(14) (a) Dürr, S.; Ertler, D.; Radius, U. *Inorg. Chem.* **2012**, *51*, 3904. (b) Zarzycki, B.; Bickelhaupt, F. M.; Radius, U. *Dalton Trans.* **2013**, *42*, 7468.

(15) Scherer, O. J.; Berg, G.; Wolmershäuser, G. *Chem. Ber.* **1995**, *128*, 635.

(16) Evans, W. J.; Ulibarri, T. A. *Inorg. Synth.* **1990**, *27*, 155.

(17) A similar compound, $[(C_5Me_4(n\text{-propyl}))_2Sm(THF)]$, was first 485 reported by Bonnet et al.: Bonnet, F.; Visseaux, M.; Barbier-Baudry, D. *J. Organomet. Chem.* **2004**, *689*, 264.

(18) Sheldrick, G. M. *Acta Crystallogr.* **2008**, *A64*, 112.

(19) (a) Ahlrichs, R.; Bär, M.; Häser, M.; Horn, H.; Kölmel, C. *Chem. Phys. Lett.* **1989**, *162*, 165. (b) Treutler, O.; Ahlrichs, R. *J. Chem. Phys.* **1995**, *102*, 346.

(20) (a) Becke, A. D. *Phys. Rev. A* **1988**, *38*, 3098. (b) Perdew, J. P. *Phys. Rev. B* **1986**, *34*, 7406. (c) Perdew, J. P. *Phys. Rev. B* **1986**, *33*, 8822.

(21) Sierka, M.; Hogekamp, A.; Ahlrichs, R. *J. Chem. Phys.* **2003**, *118*, 9136.

(22) (a) Weigend, F. *Phys. Chem. Chem. Phys.* **2006**, *8*, 1057. (b) Weigend, F.; Ahlrichs, R. *Phys. Chem. Chem. Phys.* **2005**, *7*, 3297.

(23) Dolg, M.; Stoll, H.; Savin, A.; Preuss, H. *Theor. Chim. Acta* **1989**, *75*, 173.

(24) Dehnen, S.; Bürgstein, M. R.; Roesky, P. W. *J. Chem. Soc., Dalton Trans.* **1998**, 2425.

(25) von Arnim, M.; Ahlrichs, R. *J. Comput. Chem.* **1998**, *19*, 1746.

(26) Deglmann, P.; Furche, F.; Ahlrichs, R. *Chem. Phys. Lett.* **2002**, *362*, 511.

(27) Winter, R. F.; Geiger, W. E. *Organometallics* **2003**, *22*, 1948.

(28) Veauthier, J. M.; Schelter, E. J.; Carlson, C. N.; Scott, B. L.; Re, R. E. D.; Thompson, J. D.; Kiplinger, J. L.; Morris, D. E.; John, K. D. *Inorg. Chem.* **2008**, *47*, 5841.

(29) Scherer, O. J.; Braun, J.; Walther, P.; Wolmershäuser, G. *Chem. Ber.* **1992**, *125*, 2661.

(30) Scheer, M.; Becker, U. *Chem. Ber.* **1996**, *129*, 1307.

(31) Häser, M.; Treutler, O. *J. Chem. Phys.* **1995**, *102*, 3703.

(32) Maxwell, L. R.; Hendricks, S. B.; Mosley, V. M. *J. Chem. Phys.* **1935**, *3*, 699.

(33) (a) Gamer, M. T.; Canseco-Melchor, G.; Roesky, P. W. *Z. Anorg. Allg. Chem.* **2003**, *629*, 2113. (b) Evans, W. J.; Grate, J. W.; Levan, K. R.; Bloom, I.; Peterson, T. T.; Doedens, R. J.; Zhang, H.; Atwood, J. L. *Inorg. Chem.* **1986**, *25*, 3614.

(34) In the same publication, the tetranuclear compound $[(Cp'''Co)_2(P_4)\{W(CO)_5\}_2]$ was reported. Because the number of metal atoms in this complex is higher than in **1a** and **1b**, this compound is not further considered in the discussion.

(35) For a discussion of P−P single-bond distances, see: Scheer, M.; Balazs, G.; Seitz, A. *Chem. Rev.* **2010**, *110*, 4236.

(36) The reaction of K and $[\{Cp'''Co(\mu,\eta^{2:2}\text{-}P_2)\}_2]$ was experimentally investigated and led to a color change; however, the reaction product(s) could not be characterized.

(37) Zhang, Q.; Yue, S.; Lu, X.; Chen, Z.; Huang, R.; Zheng, L.; Schleyer, P. v. R. *J. Am. Chem. Soc.* **2009**, *131*, 9789.

(38) For the isoelectronic molecule $[(CpNi)P_4CoCp]$, the same structural motif was calculated (see the Supporting Information).

(39) DFT calculation of $[(CpCo)P_4(NiCp)]$ leads to a prismatic structure analogous to that of the $[P_4(CoCp)_2]^-$ unit.

(40) Binnewies, M.; Milke, E. *Thermochemical Data of Elements and Compounds*, 2nd ed.; Wiley-VCH: Weinheim, Germany, 2002.

(41) Scheer, M.; Becker, U.; Chisholm, M. H.; Huffman, J. C.; Lemoigno, F.; Eisenstein, O. *Inorg. Chem.* **1995**, *34*, 3117.

(42) Li, T.; Kaercher, S.; Roesky, P. W. *Chem. Soc. Rev.* **2014**, *43*, 42.